

RSC Advances



This is an *Accepted Manuscript*, which has been through the Royal Society of Chemistry peer review process and has been accepted for publication.

Accepted Manuscripts are published online shortly after acceptance, before technical editing, formatting and proof reading. Using this free service, authors can make their results available to the community, in citable form, before we publish the edited article. This *Accepted Manuscript* will be replaced by the edited, formatted and paginated article as soon as this is available.

You can find more information about *Accepted Manuscripts* in the [Information for Authors](#).

Please note that technical editing may introduce minor changes to the text and/or graphics, which may alter content. The journal's standard [Terms & Conditions](#) and the [Ethical guidelines](#) still apply. In no event shall the Royal Society of Chemistry be held responsible for any errors or omissions in this *Accepted Manuscript* or any consequences arising from the use of any information it contains.

Inhibitive action of stored Olive mill wastewater (OMW) on the corrosion of copper in NaCl solution

Mohamed Masmoudi^{a*}, Chahla Rahal^a, Ridha Abdelhedi^a, Mohamed Khitouni^b, Mohamed Bouaziz^a

HPLC analysis shows that the stored OMW is greatly enriched in phenolic compounds, mainly hydroxytyrosol (HT) (2.54 g/L) and tyrosol (0.775 g/L). But, after 4 years these compounds decrease. Potentiodynamic polarization measurements show that the OMW acts as mixed-type corrosion inhibitor for copper in 3 wt NaCl solution. The exceptional effect of this inhibitor is above E_{corr} . The full passivation range greatly increases upon addition of inhibitor and increases further with increasing OMW concentration. For sufficiently-high OMW concentration, a notable absence of trans-passivation phenomenon until 2500 mV is detected and no pits are observed on the samples' surface.

*Corresponding author at: Publi Poste BP 102, 3041 Sfax, Tunisia. Tel: +216 27 75 23 24.

E-mail address: med_masmoudi@yahoo.fr (M. Masmoudi).

^aLaboratory of Electrochemistry and Environment (Lee), Sfax National Engineering School (ENIS) BPW 3038 Sfax. University of Sfax. Tunisia.

^bLaboratory of Inorganic Chemistry (Ur-11-Es-73), Faculty of Sciences of Sfax, BP 1171, 3018, University of Sfax, Tunisia.

Introduction

Olive mill wastewaters (OMWs) are dark effluents characterized by high concentrations of organic compounds, including organic acids, sugar, tannins, pectins and phenolic substances that make them phytotoxic and inhibit bacterial activity [1,2]. The composition of these effluents shows a large variability depending on several parameters such as cultivar, harvesting time, type of olives and oil extraction technology. The composition of OMW is extremely complex, as demonstrated by several authors [3-6]. The active components in OMW are known to be Oleuropein and its derivatives hydroxytyrosol and tyrosol, as well as Caffeic acid, p-coumaric acid, Oleuropeinaglycone, Lutéolin, Apigenin, fulvic acid, gallic acid, dihydroxyphenylglycol, dihydroxyphenylacetic acid, p-hydroxyphenylacetic acid.

OMWs have a direct impact on the environment due to the aesthetic degradation caused by their strong odor and dark color and due to their high organic fraction. Of all compounds, polyphenols are the most interesting due to their toxic properties and relatively slow degradation rate by specialized groups of microorganisms that may affect plants [7]. Several waste management approaches have been proposed for these effluents. Agronomic methods include their disposal in uncultivated and agricultural fields or direct disposal to surface waters [8]. However, several studies have demonstrated the negative effect that these wastes have on soil microbial populations and aquatic ecosystems [9]. Physico-chemical treatments such as decantation with lime and clay [10], coagulation-flocculation [11], electrocoagulation [12], natural evaporation and thermal concentration [13] have been proposed. Finally, composting [14] and biotechnological methods, such as biological treatment in aerated lagoons and anaerobic digestion [15], have been evaluated for their validity in reducing the polluting load of OMWs. However, in the last years OMWs have received increasing attention for the presence of high added value compounds, such as antioxidant substances and phenols OMWs can be considered as an inexpensive, potential source of high added value powerful natural antioxidants comparable to some synthetic antioxidants commonly used in the food industry. Consequently, several valorization approaches have been investigated to recover fine bioactive chemicals from OMWs that can be exploited for pharmaceutical, nourishment and cosmetic applications. Several previous works were used some natural extract, containing phenolic compounds, as a corrosion inhibitor [16-23]. Promising results were obtained in this field.

The aim of this work is to study the changes in the polyphenolic compounds, particularly hydroxytyrosol and tyrosol, on OMWs during storage and to examine these wastewaters as inhibitor for corrosion of pure copper in NaCl 3% solution.

Experimental section

Reagents and chemicals

Sodium molybdate dehydrate and organic solvents were purchased from Merck (Darmstadt, Germany). 2,2-diphenyl-1-picrylhydrazyl (DPPH), and all other chemicals were purchased from Sigma–Aldrich (St. Louis, MO). All reagents and chemicals used were of analytical grade.

Total phenols and O-diphenolic

The determination of the total phenolic compounds was performed by means of the Folin–Ciocalteu reagent. The method adopted was described in our previously work [24]. The total phenolic content was expressed as milligrams of gallic acid (GA) equivalents per liter of OMW ($y = 0.0012x - 0.0345$, $r^2 = 0.9997$).

O-diphenolic content was determined by the method described by Cert et al [25] with some modifications. This method is based on the formation of yellow complex between o-diphenols and molybdate ions. Briefly, 2 mL of sample was added to 0.5 mL of sodium molybdatedihydrate solution (5%, w / v, in a mixture ethanol / water, 1/1, v / v). The mixture was shaken. Then, after 15 min at room temperature, the absorbance was measured at 370 nm. Standards of gallic acid were prepared similarly.

Olive mill wastewater source and characteristics

The original OMW used in the present study was obtained from the discontinuous process for olive oils extraction plant located in Sfax city (Tunisia). The main characteristics of the OMW stored for 2 years were pH : 5.1 ; electrical conductivity (EC) : 9.1 dsm^{-1} ; salinity : 6.37 g L^{-1} ; COD: 93 g L^{-1} ; N : 1340 mg L^{-1} ; P: 720 mg L^{-1} ; K : 6200 mg L^{-1} ; phenols : 10020 mg L^{-1} and glucose 900 mg L^{-1} .

HPLC analysis

The identification of phenolic compounds was carried out using HPLC system (Ultimate 3000, Dionex, Germany). The HPLC system was equipped with a pump (LPG-3400SD), column oven and diode-array UV/VIS detector (DAD-3000RS). The output signal of the detector was recorded using Dionex Chromeleon™ Chromatography Data System. The separation was executed on an Inertsil ODS-4 C18 column ($5 \mu\text{m}$, $4.6 \times 150 \text{ mm}$) maintained at $35 \text{ }^\circ\text{C}$. The flow rate was 1.5 mL/min , the injection volume was $20 \mu\text{L}$ and the detection UV wavelength was set at 280 nm . The mobile phase used was 0.1% acetic acid in water (A) versus 0.1% acetic acid in acetonitrile (B) for a total running time of 25 min and the following proportions of solvent B were used for the elution: 0-5 min: 10%; 5-10 min: 10-100%; 10-20 min: 100% and 20-25 min: 100-10%.

Potentiodynamic polarization measurements

Pure copper (99.99%) was used for sample preparation. The copper electrodes for potentiodynamic polarization tests were masked by epoxy resin, leaving $10 \times 10 \text{ mm}^2$ as working surface. Prior to each test, the exposed surface was polished by means of SiC paper to # 1200, degreased with acetone, and rinsed with distilled water. The electrolyte was a 3 wt% NaCl solution prepared using distilled water. The experiments were carried out under non-stirred and naturally aerated conditions. The concentration range of OMW stored for 2 years ranges from 40 to 200 g/L .

The potentiodynamic polarization measurements were carried out in the potential range from -400 to 2500 mV , depending on the current density evolution, with a scanning rate of $0.5 \text{ mV}\cdot\text{s}^{-1}$. All measurements were repeated at least four times and good reproducibility of the results was observed. A Potentiostat Galvanostat Radiometer's Electronic controlled by the software VoltaLab was used. An electrochemical cell with a three-electrodes configuration was used; pure copper, platinum foil and a Saturated Calomel Electrode (SCE : XR110, Radiometer-Analytical) were used as a working, counter and reference electrodes, respectively.

Result and discussion

Effect of OMW storage time on phenolic compounds content

Total phenols, O-diphenols

OMW composition differs both qualitatively and quantitatively according to the olive variety, climate conditions, storage practices and the olive oil extraction process and may due to oxidation reactions. Apart from water (83-92%), the main components of OMW are phenolic compounds. Fig. 1 shows a variation of the polyphenol content during the storage time of the OMW. The sample stored for 2 years has the highest content in polyphenols, its concentration is equal to 10.02 g/L while it does not exceed 4.72 g/L for OMW stored for 2 months. The results presented in Fig. 1 show also that the content of O-diphenols of OMW analyzed varies significantly from one to another. The OMW stored for 2 years are rich in O-diphenols than stored for 2 months. Indeed, the high concentration of these compounds attained 5.35 mg/L . However, the low level was detected in the sample stored for 2 months (1.75 g/L), this could be explained by the association of monomeric phenols to the sugar and other high molecular weight compounds and to the reduced time of exposure to the

light and enzymatic reactions [26,27]. After 4 years of storage, a reduction in the concentration of total phenols and *O*-diphenols was detected, this phenomenon may be explained by the long period of OMW exposure in air and the presence of enzymes secreted by microorganisms. In addition, phenols are reactive chemical species, vulnerable to oxidation, conjugation, hydrolysis, polymerization, and complexation [4].

Identification and quantification of phenolic monomers in OMW

A reversed-phase high-performance liquid chromatographic technique was used to identify and quantify the major phenolic compounds of OMW. For this purpose, standards mixture solution of phenolic compounds was analyzed. Sample concentrations were calculated based on peak areas compared to those of each of the external standards as described in the Materials and methods section. Representative chromatograms of OMW, after (a) 2 months, (b) 2 years and (c) 4 years of storage, obtained after HPLC analysis is given in Fig. 2. These chromatograms show several peaks corresponding to different phenolic monomers. From the retention time comparison and with co-elution with standards, it was deduced that the stored OMW were greatly enriched in HT and slightly in tyrosol. This may be explained by the hydrolysis of the secoiridoid derivatives having in part in their structure HT and tyrosol [26].

The changes in the HT and tyrosol concentrations during the storage times of OMW are given in Table 1. As expected, HT is the major polyphenol compounds in the stored OMW, it attains 2.54 g/L after 2 year of storage. However, the highest concentration of tyrosol does not exceed 0.775 g/L after the same period. The analysis of the sample collected after 4 years of storage shows that the content of HT and tyrosol decreased, which may be due to oxidation, polymerization and complexation reactions. The obtained result correlates with that previously described [4].

Effect of OMW concentration on the electrochemical behavior.

Potentiodynamic polarization measurements.

Fig. 3a shows the typical potentiodynamic polarization curve of copper in aerated NaCl 3wt % aqueous solution (i.e., the blank). This curve reveals that below -320 mV the cathodic curve for the pure copper showed nearly flat current density, indicating diffusion-controlled cathodic reactions. It is well known that the cathodic copper reactions in NaCl solution should be the reduction of water (1) and the reduction of oxygen (2) when it approaches the corrosion potential [28,29]:



It could be observed that the pH value of the solution after the electrochemical experiments is a little higher than that before the experiment.

The anodic process of copper could be explained as follows [29,30]:

First, due to the oxidation of Cu(0) to Cu(I) (3), the current density increases from lower anodic potential to a critical passivation value (J_{cp}).



Then, under the attack of the Cl^- , Cu(I) is rapidly transformed to an insoluble film CuCl (4). The current density decreases from J_{cp} to full passivation current density (J_{pas}).



Finally, due to its poor stability, CuCl is immediately transformed to the soluble cuprous complex CuCl_2^- (5). The current density rapidly increases again from J_{pas} to higher anodic potential. A very small full passivation range (7 mV/ECS) was observed in the blank chloride solution. Thus, the dissolution of copper is occurring step by step.



However, according to some authors, other corrosion products could be also formed, such as Cu_2O , CuO , $\text{Cu}(\text{OH})_2$ [31-33].

The cathodic and anodic polarization curves of copper in NaCl 3wt % solutions devoid of and containing different concentrations of OMW stored for 2 years are represented in Fig. 3. Inspection of this figure reveals that the potentiodynamic polarization curves are slightly shifted toward more negative potential and less current density upon addition of OMW, containing principally hydroxytyrosol (HT) as mentioned above. This result shows the inhibitive action of the OMW toward corrosion of copper. The electrochemical parameters such as corrosion potential (E_{corr}), corrosion current density (J_{corr}), cathodic (β_c) and anodic Tafel (β_a) slopes, polarization resistance (R_p), corrosion rate (CR) and inhibition efficiency (IE , %) are listed in Table 2.

The values of J_{corr} and E_{corr} are obtained from the extrapolation of anodic and cathodic Tafel lines located next to the linearized current regions. The R_p values are calculated as follows [28],

$$R_p = \frac{B}{J_{\text{corr}}} \quad (6)$$

Here, B is a constant that is calculated by using Stern–Geary equation [28],

$$B = \frac{\beta_c \beta_a}{2.303(\beta_c + \beta_a)} \quad (7)$$

The values of corrosion rate (CR , millimeters per year ($\text{mm}\cdot\text{y}^{-1}$)) are calculated using the expression [34],

$$CR = 3.268 \times 10^3 \frac{J_{\text{corr}} \cdot MW}{\rho \cdot Z} \quad (8)$$

where MW is molecular weight of copper in g, ρ is the density of Cu in $\text{g}\cdot\text{cm}^{-3}$ ($=8.92$) and Z is the number of electrons transferred in the corrosion reaction; $Z = 2$ in the case of Cu reaction. While, the inhibition efficiency (IE , %) of the OMW effect on corrosion resistance was calculated using the following equation (9) [35]:

$$(IE)\% = \left(1 - \frac{J'_{\text{corr}}}{J_{\text{corr}}} \right) \times 100 \quad (9)$$

where J_{corr} and J'_{corr} are the corrosion currents density in absence and presence of wastewater, respectively.

Inspection of Table 2 and Fig. 3 reveals that the values of the anodic Tafel slop remain almost unchanged upon the addition of the HT and both cathodic (β_c) and anodic Tafel (β_a) depend slightly on the OMW concentration. It indicates that the OMW act as a corrosion inhibitor suppressing both anodic and cathodic reactions. This compound affects the anodic dissolution of copper as well as the cathodic reduction reactions. Therefore, it could be concluded that the phenolic compound adsorb (physically and/or chemically) onto both anodic and cathodic sites of the copper surface. In addition, compared with the blank, the E_{corr} values move slightly in the negative direction, and all the displacement are less than 35 mV/SCE, which confirm that the OMW acts as mixed-type corrosion inhibitor [36]. Further inspection of Table 2 reveals that the J_{corr} value of the bare copper ($15.85 \mu\text{A}\cdot\text{cm}^{-2}$) is reasonable compared with the literature data of copper corrosion rates in 3wt % NaCl solutions [37–39]. This value decreases sharply upon addition of the inhibitor, leading to a decrease in the corrosion rate and an increase in the polarization resistance and the inhibition efficiency. Nevertheless, all the corrosion parameters depend slightly on the OMW concentration, as shown in Fig. 4. This behavior reflects the OMW ability to inhibit the corrosion of copper in chloride solution.

Fig. 3 also shows that the copper in the blank solution reaches passivity in a typical active-passive transition. The specimen in wastewater chloride solution featured much wider potential range of full passivation, which provides additional protection at high values of anodic potential. The values of some other parameters obtained from Fig. 3 are listed in Table 3. The comparison of anodic behaviour of the copper has shown that the addition of the OMW performs an improvement in corrosion resistance, especially above E_{corr} value (uniform corrosion). Indeed, a further increase in potential's values towards positive direction has revealed the beginning of corrosion in all specimens, related to dissolution of the metal. The specimens get successively covered with a passive film until the beginning of critical passivation potential, E_{cp} , at the critical current density of passivation, J_{cp} . Above the value of E_{cp} , a sudden decrease in current density appears, below the critical value, J_{cp} , to the value of full passivation start current density, J_{pos} , and the potential of full passivation start, E_p , what is related to passive film sealing (increasing its thickness). The shift of E_{cp} and E_p values towards negative potentials proves higher corrosion resistance of the copper upon addition of inhibitor. Nevertheless, all the corrosion parameters are almost independent on the OMW concentration. The lower value of full passivation current density, J_{pos} , in the presence of OMW, proves a better tightness on the passive layer formed on the copper surface. In the fully passive range, the current density is independent of the potential. When the potential of full passivation finishes, E_{tp} is reached. After this, the passive film continuity is damaged and the metal gets trans-passivated. Further inspection of Table 3 reveals also that the trans-passivation potential, E_{tp} , greatly increases upon addition of inhibitor and increases further with increasing inhibitor concentration. Fig. 5 shows more the evolution of the passive range, characterized by the difference between E_{tp} and E_{pos} ($\Delta E = E_{tp} - E_{pos}$) as a function of OMW concentration. It is observed that the passive range increases upon addition of inhibitor. Then, it increases almost linearly with the increasing of the inhibitor concentration. Above the trans-passivation start, a sudden increase in the current density has been observed (Fig. 3), along with the evolution of molecular oxygen and the return to the active area, where metal's dissolution took place.

Adsorption behavior

It is widely accepted that organic molecules inhibit corrosion by adsorption at the metal/solution interface. The adsorption of compounds can be described by two main types of interaction: physical adsorption and chemisorption [40]. A direct relationship between inhibition efficiency (IE , %) and the degree of surface coverage by the adsorption molecules (θ).

Therefore, θ is calculated using the relation $\theta = IE/100$, and the calculated values are added in Table 2. The degree of surface coverage for the different concentrations of HT has been evaluated from the potentiodynamic polarization measurements.

As described above, the major constituents of the OMW is the hydroxytyrosol (HT). The latter may play the major role in the inhibition process. Thus, the concentrations used in the adsorption isotherm diagram (Fig. 6) were the HT concentrations in the different test solutions. Surface coverage data were tested by fitting to series of adsorption isotherm including Temkin, Freundlich, Flory-Huggins, Langmuir, and Frumkin isotherms and the best fit was obtained using the Langmuir adsorption isotherm, which can be expressed by the following equation (10) [17,41]:

$$\frac{C}{\theta} = \frac{1}{K_{\text{ads}}} + C \quad (10)$$

Where θ is the degree of the coverage on the metal surface, C is the HT concentration (mmol.L^{-1}) and K_{ads} is the equilibrium constant of adsorption-desorption process (mol^{-1}L). The latter is related to the standard free energy of adsorption (ΔG_{ads}^0) according to relation [17,42]:

$$\Delta G_{\text{ads}}^0 = -RT \ln(55.5K_{\text{ads}}) \quad (11)$$

where R is the molar gas constant ($8.314 \text{ J mol}^{-1}\text{K}^{-1}$) and T is the absolute temperature (K).

Fig. 6 represents the Langmuir adsorption plot of HT on the copper surface. The best fitted straight line is obtained for the plot of C/θ versus C . The correlation coefficient ($R^2 = 0.997$) is very close to one and confirms that the adsorption of HT on the copper surface in NaCl solution obeys the Langmuir adsorption isotherm. The latter assumes that the adsorbed molecules occupy only one site and there are no interactions between the adsorbed species [43]. The value of ΔG_{ads}^0 was calculated as $-30.50 \text{ kJ mol}^{-1}$. The negative value of standard free energy of adsorption indicates the strong interaction and stability of the adsorption layer with the copper surface [44]. Generally, the magnitude of Standard free energy of adsorption is around -20 kJ mol^{-1} or less negative, which can be assumed that an electrostatic interaction exists between the inhibitor and the charged metal surface (i.e. physical adsorption); those around -40 kJ mol^{-1} or more negative involve charge sharing or transfer from the inhibitor molecules to the metal surface to form a coordinate type of bond (i.e. chemical adsorption) [17]. Therefore, the obtained value of ΔG_{ads}^0 suggests a strong physical adsorption of HT onto the copper surface in NaCl solution [17,45].

The phenolic compound adsorbs on the copper surface through the lone pairs of electrons of the oxygen atoms forming a covering film. Inspection of the chemical structure in Fig. 7 reveals that the oxygen atoms almost surround the aromatic rings of the HT. This arrangement of the oxygen atoms may lead to the conclusion that this phenolic compound is forced to be adsorbed horizontally onto the copper surface. This adsorption gives rise to a large covered surface area with a small number of adsorbed molecules. Therefore, high inhibition efficiency could be obtained by relatively low concentrations of the HT.

OMW storage time effect

Fig. 8 shows potentiodynamic polarization curves of copper in OMW stored for (b) 2 months, (c) 2 years and (d) 4 years. All test solutions containing 3 wt% NaCl. The curve of pure copper is also included in the figure for comparison, ((a) blank). It can be seen from Fig. 8 that all the wastewaters have a relatively beneficial effect on the uniform corrosion of pure copper but its effect on passivation range is very interesting. Above E_{pas} value, three types of electrochemical behaviour appeared in the case of OMW stored for 2 months: (i) full passivation, (ii) defective passivation: as the increase of the current densities with increasing potential is small and the values reached not very high, it is assumed that this behaviour is associated with the presence of defective sites in the passivation film covering the metal and (iii) trans-passivation phenomena: pitting corrosion can take place. As for the OMW stored for 2 and 4 years, we remark a notable absence of trans-passivation phenomenon until 2500 mV. Better passive film continuity is observed, and the copper surface is completely protected against corrosion, especially, in the OMW stored for 2 years. It should be noted, in this case, that the defective passivation zone reduced sharply.

Conclusions

The main conclusions of this study are summarized below:

- The stored OMWs are greatly enriched in phenolic compound, mainly HT and tyrosol. But, after 4 years (a sufficiently long period of storage) the concentration of these compounds decreases.
- The OMW acts as a mixed-type corrosion inhibitor. The molecules of this inhibitor physically adsorbed onto both anodic and cathodic sites of the copper surface.
- The full passivation range greatly increases upon addition of inhibitor and increases further with increasing OMW concentration.

- Above E_{pas} , three types of electrochemical behaviour appear in the case of OMW stored for 2 months: (i) full passivation, (ii) defective passivation and (iii) trans-passivation. For the OMW stored for 2 or 4 years, we remark a notable absence of trans-passivation phenomenon until 2500 mV.

Acknowledgement

The authors thank Professor Skander ABID, Teacher of English, for reviewing the paper.

References

1. A.R. Cormenzana, B.J. Jiménez, M.P. Garcia-Pereja, *Int. Biodet. Biodeg.*, 1996, **38**, 283.
2. A. Rozzi, F. Malpei, *Int. Bio. Biodeg.*, 1996, **38**, 135.
3. C. Plaza, N. Senesi, G. Brunetti, D. Mondelli, *Biores. Techno.*, 2007, **98**, 1964.
4. H.K. Obied, M.S. Allen, D.R. Bedgood, P.D. Prenzler, K. Robards, R. Stockmann, *J. Agri. Fo. Chemi.*, 2005, **53**, 823.
5. L.S. Artajo, M.P. Romero, M.J. Motilva, *J. Sci. Food Agric.*, 2006, **86**, 518.
6. A. El Hadrami, M. Belaqiz, M. El Hassni, *J. Agron.*, 2004, **3**, 247.
7. I.S. Arvanitoyannis, A. Kassaveti, S. Stefanatos, *Cri. Rev. Fo. Sci. Nutri.*, 2007, **47**, 187.
8. M. Rinaldi, G. Rana, M. Intronza, *Fie. Cro. Res.*, 2003, **84**, 319.
9. M.D. Greca, P. Monaco, G. Pinto, A. Pollio, L. Previtera, F. Temussi, *Bul. Envi. Conta. Toxicol.*, 2001, **67**, 352.
10. E.S. Aktas, I. Sedat, L. Ersoy, *Wat. Resear.* **35**, 2336 (2001)
11. L.M. Nieto, G. Hodaifa, S. Rodríguez, J.A. Giménez, J. Ochando, *Cle. So. Air Wat.*, 2011, **39**, 949.
12. H. Inan, A. Dimoglo, H. Simsek, M. Karpuzcu, *Sep. Puri. Techno.*, 2004, **36**, 23.
13. R. Jarboui, M. Chtourou, C. Azri, N. Gharsallah, E. Ammar, *Bio. Techn.*, 2010, **101**, 5749.
14. E.K. Papadimitriou, I. Chatjipavlidis, C. Balis, *Env. Techn.*, 1997, **18**, 101.
15. P. Paraskeva, E. Diamadopoulos, *J. Chemi. Techn. Biot.*, 2006, **81**, 1475.
16. H. Z. Alkhatlan, M. Khan, M. M. S. Abdullah, A. M. AlMayouf, A.Y. Badjah-HadjAhmed, Z. A. AlOthman, A. A. Mousa, *RSC Adv.*, 2015, **5**, 54283.
17. A.A. Farag, T.A. Ali, *J. Ind. Eng. Chemi.*, 2015, **21**, 627.
18. A. Abdel Nazeer, K. Shalabi, A. S. Fouda, *Res. Chem. Intermed.*, 2015, **41**, 4833.
19. M. Prabakaran, S.H. Kim, V. Hemapriya, M. Chung, *Res. Chem. Intermed.*, 2015, **xx**, xxx.
20. L. Afia, R. Salghi, E.H. Bazzi, A. Zarrouk, B. Hammouti, M. Bouri, H. Zarrouk, L. Bazzi, L. Bammou, *Res Chem Intermed.*, 2012, **38**, 1707.
21. K.K. Anupama, J. Abraham, *Res. Chem. Intermed.*, 2013, **39**, 1067.
22. T. Ibrahim, H. Alayan, Y. Al Mowaqet, *Prog. Org. Coat.*, 2012, **75**, 456.
23. A. Khadraoui, A. Khelifa, H. Hamitouche, R. Mehdaoui, *Res. Chem. Intermed.*, 2014, **40**, 961.
24. F. Mraicha, M. Ksantini, O. Zouch, M. Ayadi, S. Sayadi, M. Bouaziz, *Fo. Chemi. Tox.*, 2010, **48**, 3235.
25. S. Arranz, R. Cert, J.P. Jiménez, A. Cert, F.S. Calixto, *Fo. Chemi. Tox.*, 2008, **110**, 985.
26. M. Feki, N. Allouche, M. Bouaziz, A. Gargoubi, S. Sayadi, *Eur. J. Lip. Sci. Techno.*, 2006, **108**, 1021.
27. A. Ranalli, L. Lucera, S. Contento, *J. Agri. Fo. Chemi.*, 2003, **51**, 7636.
28. A. Ehsani, M.G. Mahjani, R. Moshrefi, H. Mostaanzadeh, J.S. Shayeh, *RSC Adv.*, 2014, **4**, 20031.
29. M.A. Amin, K.F. Khaled, *Corro. Sci.*, 2010, **52**, 1194.
30. E.S.M. Sherif, A.M. El Shamy, M.M. Ramla, A.O.H. El Nazhawy, *Mat. Chemi. Physi.*, 2007, **102**, 231.
31. M. Masmoudi, M. Abdelmouleh, R. Abdelhedi, *Spec. Ac. Pat A: Mole. Biom. Spect.*, 2014, **118**, 643.
32. M. Scendo, *Corro. Sci.*, 2008, **50**, 1584.
33. G. Kear, B.D. Barker, F.C. Walsh, *Corro. Sci.*, 2004, **46**, 109.
34. V. Ezhil Selvi, H. Seenivasan, K.S. Rajam, *Surf. Coat. Techno.*, 2012, **206**, 2199.
35. H. Allachi, F. Chaouket, K. Draou, *J. Alloy. Comp.*, 2010, **491**, 223.
36. H. Tian, W. Li, B. Hou, *Int. J. Electro. Sci.*, 2013, **8**, 8513.
37. K.F. Khaled, *Mater. Chemi. Phys.*, 2008, **112**, 104.
38. H. Otmacic, E. Stupnisek-Lisac, *Electro. Acta.*, 2003, **48**, 985.
39. V. Shinde, S.R. Sainkar, P.P. Patil, *Corro. Sci.*, 2005, **47**, 1352.

40. M.A. Amin, S.S. Abd El Rehim, H.T.M. Abdel-Fatah, *Corro. Sci.*, 2009, **51**, 882.
41. P. Roy, T. Maji, S. Dey, D. Sukul, *RSC Adv.*, 2015, **5**, 61170
42. A.R. Hosein Zadeh, I. Danaee, M.H. Maddahy, *J. Mater. Sci. Technol.*, 2013, **29**, 884.
43. J. Aljourani, M.A. Golzar, K. Raeissi, *Mater. Chemi. Phys.*, 2010, **121**, 320.
44. Z. Jia, J. Liu, Q. Wang, S. Li, Q. Qi, R. Zhu, *J. Alloy. Comp.*, 2015, **622**, 587.
45. I. Ahamad, R. Prasad, M.A. Quraishi, *Corro. Sci.*, 2010, **52**, 3033.

Figure Captions

Fig. 1. Total phenols and O-diphenols content in OMW stored for different times.

Fig. 2. HPLC chromatograms of OMW after (a) 2 months, (b) 2 years and (c) 4 years of storage.

Fig. 3. Potentiodynamic polarization curves of copper in NaCl 3wt % solutions devoid of and containing different concentrations of OMW.

Fig. 4. Corrosion rate and inhibition efficiency of copper in NaCl 3wt % as function of OMW concentration.

Fig.5. Relation between passive range and OMW concentration.

Fig. 6. Langmuir adsorption isotherm of HT on the copper surface.

Fig. 7. Chemical structure of the hydroxytyrosol.

Fig. 8. Potentiodynamic polarization curves of copper in NaCl 3wt % solutions devoid of and containing OMW stored for different times.

Table 1

Evolution of HT and tyrosol concentrations during the storage times of OMW.

	HT (g/L)	Tyrosol(g/L)
OMW stored for 2 months	0.98 ± 0.16	0.230 ± 0.09
OMW stored for 2 years	2.54 ± 0.20	0.775 ± 0.10
OMW stored for 4 years	1.43 ± 0.14	0.280 ± 0.07

Table 2

Electrochemical parameters and degree of surface coverage obtained from potentiodynamic polarization curves of copper in NaCl 3wt % solutions devoid of and containing different concentrations of OMW stored for 2 years.

Solutions		Parameters							
OMW conc. (g/L)	HT conc. (mmol/L)	E_{corr} (mV/SCE)	$-\beta_c$ (mV/dec)	β_a (mV/dec)	J_{corr} ($\mu\text{A}/\text{cm}^2$)	R_p ($\text{k}\Omega\text{cm}^2$)	CR (mm/year)	IE. (%)	θ
Blank	Blank	-218	101	55	15.85	0.97	0.184	-	
40	0.66	-233	175	67	3.80	5.54	0.044	76.03	0.760
80	1.32	-240	163	60	3.98	5.52	0.046	74.89	0.749
120	1.98	-241	181	62	3.39	5.91	0.039	78.61	0.786
160	2.64	-248	150	60	2.45	7.75	0.028	84.54	0.845
200	3.30	-253	180	59	2.51	7.79	0.029	84.16	0.842

Table 3

Characteristic passivation parameters obtained from potentiodynamic polarization curves of copper in NaCl 3wt % solutions devoid of and containing different concentrations of OMW stored for 2 years.

Solutions		Parameters			
OMW conc. (g/L)	E_{cp} (mV/SCE)	J_{cp} (mA.cm ⁻²)	E_p (mV/SCE)	J_p (mA.cm ⁻²)	E_{tp} (mV/SCE)
Blank	7	7.94	40	1.32	47
40	1	6.31	26	0.62	109
80	1	6.17	27	0.55	130
120	3	6.03	32	0.63	184
160	-8	6.46	31	0.56	275
200	0	5.89	31	0.53	483

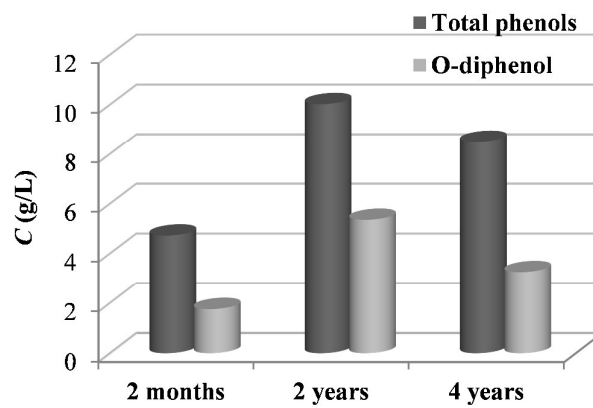


Fig. 1. Total phenols and *O*-diphenols content in OMW stored for different times.

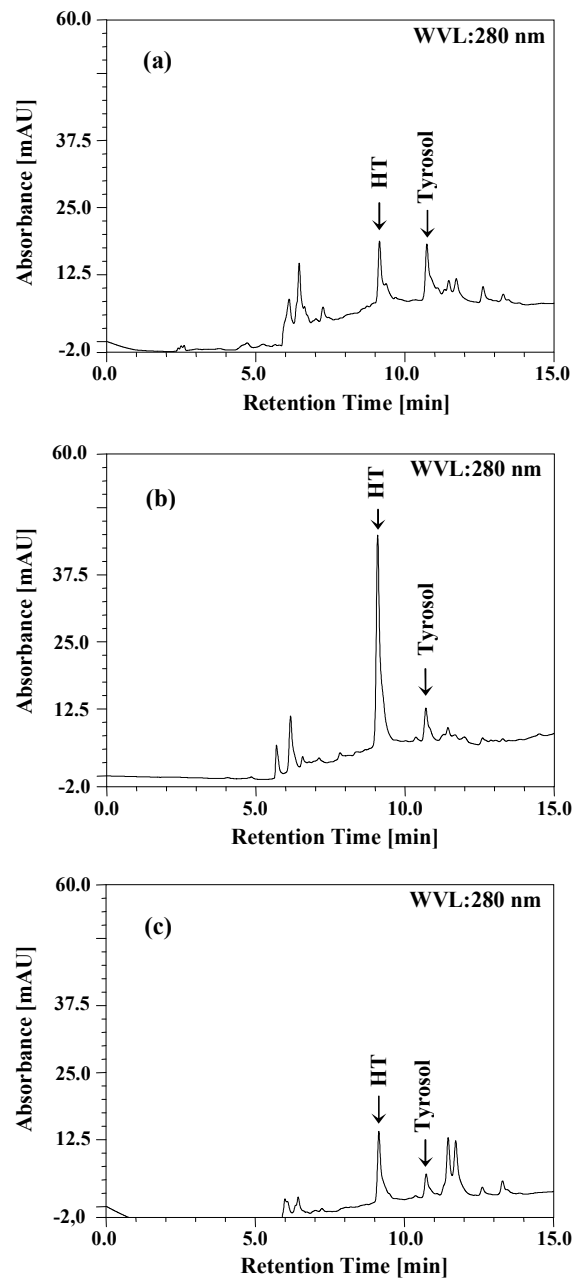


Fig. 2. HPLC chromatograms of OMW after (a) 2 months, (b) 2 years and (c) 4 years of storage.

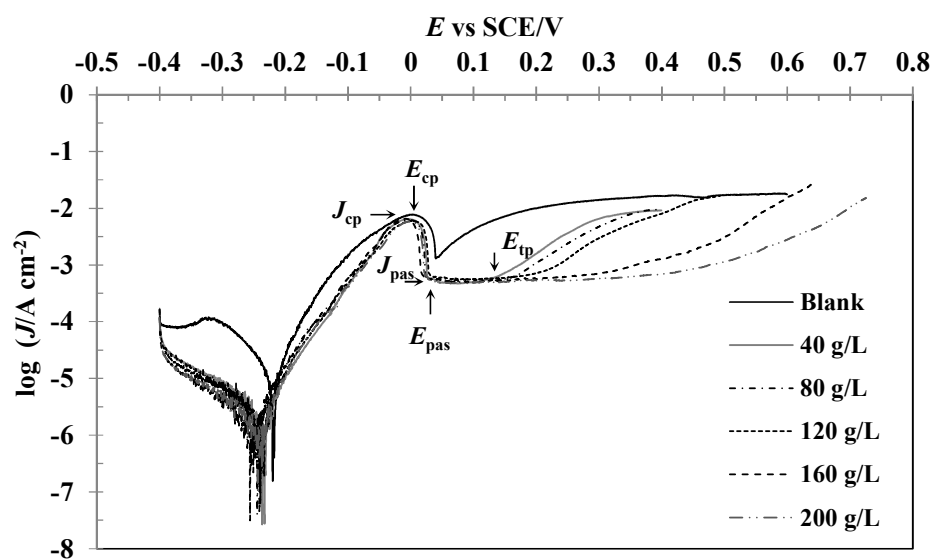


Fig. 3. Potentiodynamic polarization curves of copper in NaCl 3wt % solutions devoid of and containing different concentrations of OMW.

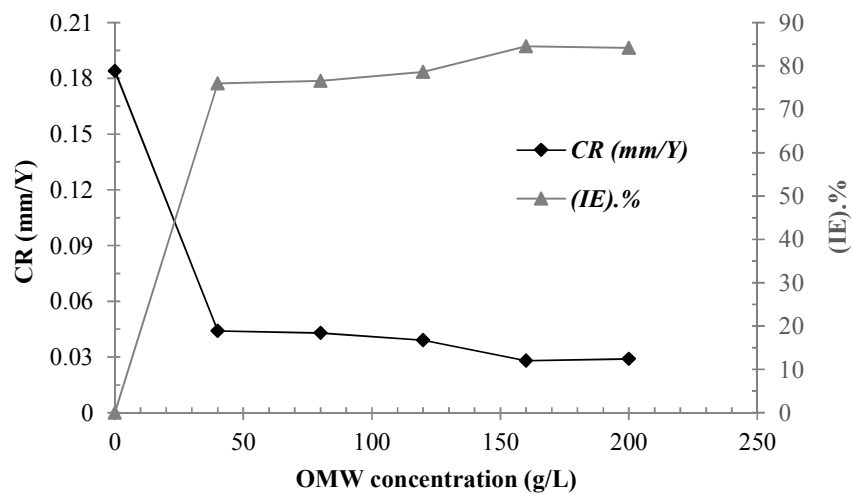


Fig. 4. Corrosion rate and inhibition efficiency of copper in NaCl 3wt % as function of OMW concentration.

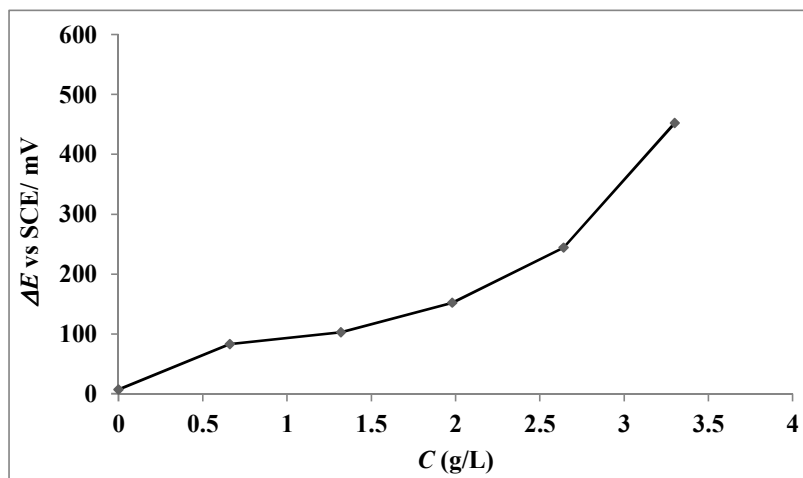


Fig.5. Relation between passive range and OMW concentration.

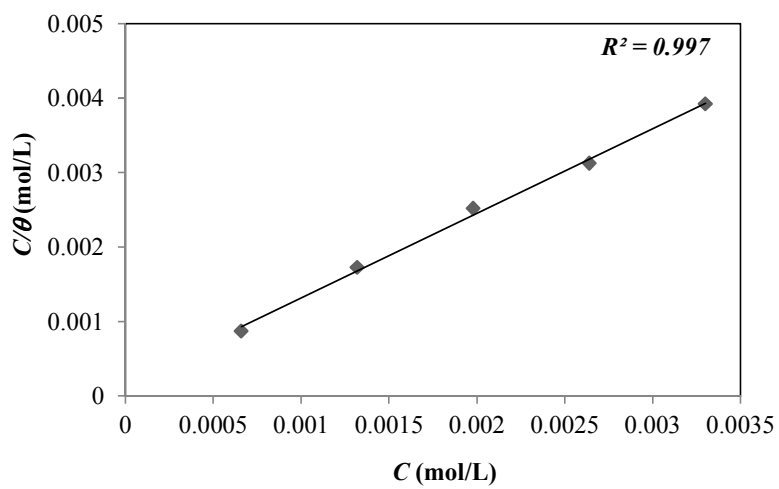


Fig. 6. Langmuir adsorption isotherm of HT on the copper surface.

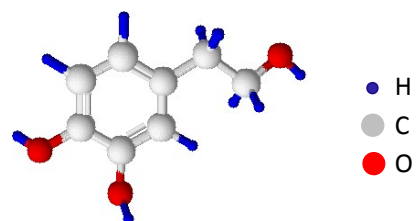


Fig.7. Chemical structure of the hydroxytyrosol.

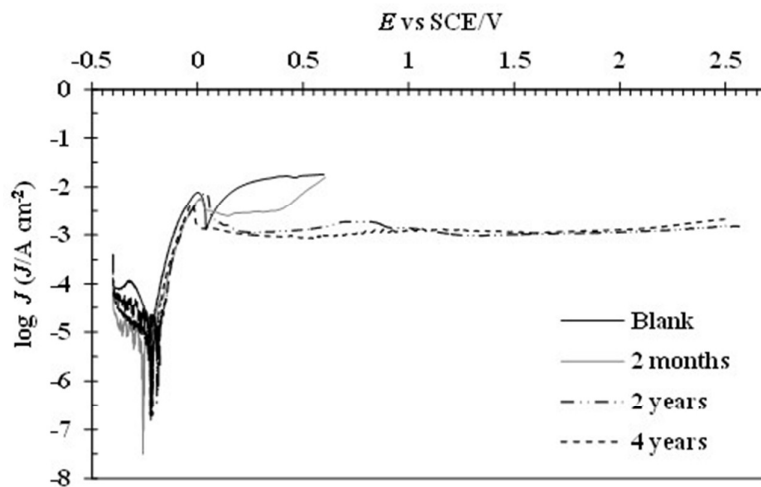


Fig. 8. Potentiodynamic polarization curves of copper in NaCl 3wt % solutions devoid of and containing OMW stored for different times.